*Progress In Electromagnetics Research, Vol. 114, 369–381, 2011*

# EMPIRICAL MINIATURIZATION ANALYSIS OF INVERSE PARABOLIC STEP SEQUENCE BASED UWB ANTENNAS

**R. Saleem and A. K. Brown**

Microwave and Communication Systems (MACS) Research Group
School of Electrical and Electronic Engineering
The University of Manchester
Oxford Road, M13 9PL, Manchester, UK

**Abstract**—In this paper we develop an empirical approach to the design of Ultra Wideband (UWB) antennas employing the Inverse Parabolic Step Sequence (IPSS). The relationships developed can be used to miniaturize the antenna and achieve a good impedance match over the UWB bandwidth. The overall aim of this process is to give a good starting point for detailed numerical optimizations. We will illustrate the use of these formulae in three different designs of IPSS-based antennas. A low loss duroid substrate of loss tangent, $\tan\delta$, 0.0009, low relative permittivity 2.2 and thickness 1.575 mm is used to simulate these planar monopole antennas in Ansoft High Frequency Structure Simulator (HFSS).

## 1. INTRODUCTION

UWB system may be defined as any radio system that has a bandwidth, larger than 25 percent of its center frequency or a bandwidth of more than 500 MHz [1], with reference to a Voltage Standing Wave Ratio (VSWR) of $< 2$. UWB technology has significant potential due to its employability in radar, remote sensing, geolocation and most importantly in high speed Wireless Personal Area Networks WPAN's. These short range networks typically operate within a range of $< 10$ meters. Speeds which extend up to one Gbps, low power usage and minimum interference levels are the promising features. A 7.5 GHz spectrum, i.e., from 3.1 GHz to 10.6 GHz has been opened for UWB by

*Received 28 January 2011, Accepted 3 March 2011, Scheduled 4 March 2011*
Corresponding author: Rashid Saleem (rashid.saleem@postgrad.manchester.ac.uk).

the Federal Communications Commission (FCC) since 2002 [2] whereas European Commission has allowed 6.0 GHz to 8.5 GHz bandwidth.

The two contesting radios for UWB application are multiband orthogonal frequency division multiplexing, MB-OFDM, and Direct Sequence, DS UWB. For MB-OFDM, the spectrum is equally divided into 14 sub-bands of bandwidth 528 MHz each [3]. A first generation MB-OFDM device is designed to frequency hop with equal probability in the first three sub-bands centered at 3432, 3960 and 4488 MHz. On the other hand, DS-UWB is supposed to work in two bands only, i.e., low band and high band. The low band covers 3.1 to 4.9 GHz part of the spectrum whereas the high band covers 6.2 to 9.7 GHz. A first generation DS-UWB transceiver operates in the lower frequency band.

Depending on the communication system requirements, the antenna has to be designed with certain features. UWB antennas may require not only impedance matching but also phase linearity for minimum distortion of the input pulse. In addition, low cost and ease of manufacturing are the other important points. Last but not the least is the size of the antenna. This is important not only because of ease of portability or space constraints, but also that relatively large three dimensional monopole-like UWB antennas have high electric near fields which cause unwanted coupling to the nearby objects [4, 5]. Not only the antenna but also their feed networks can have adverse effects. UWB antennas having an unbalanced feed network can experience significant coupling even from any high-dielectric objects in the near vicinity [6].

The shortcomings which give rise to unwanted coupling are not present when compact planar UWB antennas are employed. These antennas form a specialized class which have been researched extensively in literature [1, 5, 7–18]. Being planar and small size they are easily packaged into a communication device. For feeding the planar monopole antennas either microstrip line or CPW have been commonly employed in the existing literature. The CPW has an advantage of lower loss over the microstrip line. In addition, shunt and series connections can be made on the same side as the antenna in CPW, avoiding via or holes in case of the microstrip line [17].

In two recent conference papers [19, 20] the authors had proposed two UWB antennas. In [19] an antenna geometry suitable for UWB application is presented via the use of an Inverse Parabolic Step Sequence (IPSS). A smaller physical size is demonstrated in [20] where the authors further the concept of IPSS. In this paper we will discuss the measurement results of these two IPSS UWB antennas. We will discuss the miniaturization process and propose a new antenna resulting from further miniaturization.

The rest of this paper in organized as follows. Section 2 discusses

the measurement results of the antennas whose simulation only results have been presented in [19, 20]. Section 3 will give details about an empirical miniaturization process and present a new antenna which results from this process. Section 4 discusses an electrical miniaturization limit of the IPSS based antennas. Finally Section 5 will conclude the paper.

## 2. IPSS ANTENNAS: SIMULATION VS. MEASUREMENTS

Previously we presented UWB antennas which are physically as well as electrically small. The largest dimension of the antenna element presented in [19] is $0.27\lambda$ whereas the largest dimension of the antenna in [20] is $0.16\lambda$. The reference $\lambda$ is the wavelength of the UWB frequency at 3 GHz.

For the antennas feed we use conventional coplanar waveguide (CPW). We then employ our proposed curve sequence in the transition region from the CPW feedline to the main radiating element. The total number of resonant frequencies increases in the VSWR response when we use multi-point curves instead of straight lines and hence the overall match improves. The preference of curves over straight lines to enhance the impedance bandwidth has been clearly demonstrated by Kan et al. in [21]. They proposed novel planar CPW fed yagi antenna whose driven as well as director elements are elliptically shaped instead of being linear to improve the VSWR bandwidth. Similarly, Mehdipour et al. [22] proposed yet another CPW fed planar UWB antenna. The transition region connecting CPW to the main radiation element is a tapered structure formed by ellipses for an enhanced match. The antennas in Fig. 1 are simulated and fabricated on low loss duroid 5880 substrate of relative permittivity 2.2 and $\tan\delta = 0.0009$. The characteristic impedance of the CPW for both the antennas is $50\,\Omega$. The IPSS antenna [19] is shown in Fig. 1(a). The dimensions are 27.1 mm × 30 mm × 1.575 mm. The parabolic step generating sequence marked as 1–4 on the antenna has the following set of equations:

$$\begin{array}{ll} y_1(x) = x^2 + 3.31, & 2.7 \le |x| \le 2.982 \\ y_2(x) = 0.25\sqrt{x} + 11.77, & 2.982 \le |x| \le 5.048 \\ y_3(x) = x^2 - 13.15, & 5.048 \le |x| \le 5.170 \\ y_4(x) = \sqrt{x} + 11.31, & 5.170 \le |x| \le 7.115 \end{array} \quad (1)$$

The central feed of the waveguide is 3.62 mm × 10.6 mm and is separated from the ground planes by 0.39 mm.

The Reflected IPSS antenna [20], is shown in Fig. 1(b). The dimensions are 16 mm × 16 mm × 1.575 mm. Again it has a parabolic

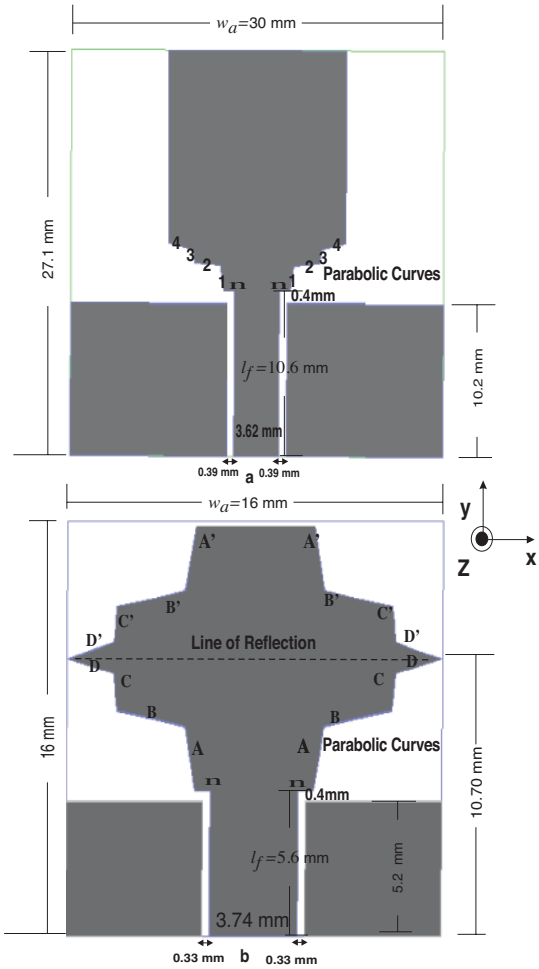


**Figure 1.** (a) IPSS Antenna. (b) Reflected IPSS Antenna

step generating function set given as follows:

$$\begin{aligned} y_A(x) &= x^2 - 0.65, & 2.5 \le |x| \le 2.958 \\ y_B(x) &= 0.833\sqrt{x} + 6.668, & 2.958 \le |x| \le 5.856 \\ y_C(x) &= x^2 - 25.61, & 5.856 \le |x| \le 5.975 \\ y_D(x) &= 1.614\sqrt{x} + 6.159, & 5.975 \le |x| \le 7.933 \end{aligned} \tag{2}$$

Reflection of the entire set of curves given by Equation (2) in the horizontal line $y = 10.70$ then yields the curves marked as $A'$-$D'$. The central feed of the waveguide is 3.74 mm $\times$ 5.6 mm and is separated from the ground planes by 0.33 mm.

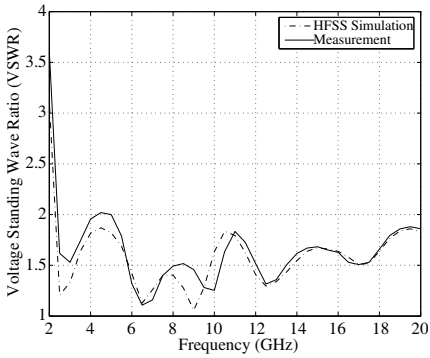


**Figure 2.** IPSS UWB antenna: Simulation vs. Measurement.

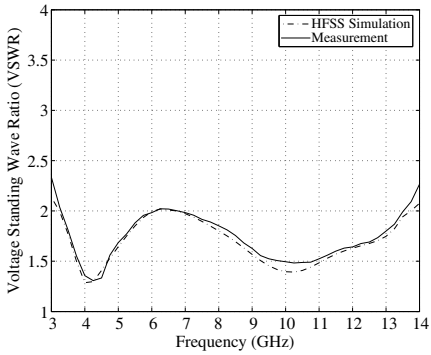


**Figure 3.** Reflected IPSS UWB antenna: Simulation vs. Measurement.

The input VSWR measurement vs. simulation results for the antennas are given in Fig. 2 and Fig. 3. As can be observed the simulation and measurement results are in close agreement. For the IPSS antenna, previously reported performance was for the frequency range 3–16 GHz, whereas now the simulation and measurement results both show an extended match up to at least 20 GHz. The connector used is a standard sma pcb with maximum operational frequency of 18 GHz.

The choice of Rogers duroid 5880, which is PTFE-based low relative permittivity and low loss substrate, is made to ensure minimum dispersion and losses, over the entire impedance bandwidth, in general, and higher frequencies in particular. A different CPW feedline-to-antenna transition region geometry would be required to provide the same impedance match for a different substrate because of different relative permittivity and loss tangent. Quite expectedly, the Reflected IPSS geometry when simulated on epoxy based FR-4 substrate (relative permittivity 4.4 and loss tangent 0.02) shows predominant mismatch over the same bandwidth. The IPSS method when applied to a different substrate would yield a different set of equations. The equations in that case would have same alternating exponents of $x$ as in Equation (1), i.e., 2 and 1/2 but the coefficients/stretch-factors and constants/y-intercepts would be different to achieve the same match. For the antennas in Figs. 1(a) and (b) these coefficients of exponents and the corresponding constants are derived after exhaustive simulations runs. However, from the trends observed in the coefficients and constants of these two antennas we aim to predict the ranges of these coefficients and constants for subsequently miniaturized antennas

on duroid 5880 substrate. Of course, the empirical miniaturization analysis of other IPSS-based UWB antenna families fabricated on different substrates would yield distinct ranges of these coefficients and constants.

## 3. MINIATURIZATION PROCEDURE

Miniaturization of UWB antennas is clearly important for many applications. Here we derive empirically based formulae to enable the size of our reference antenna to be reduced and still maintain a reasonable input VSWR. We take as our reference the geometry of Reflected IPSS antenna shown in Fig. 1(b). UWB Antenna elements formed entirely by a single type of mathematical function have been presented mostly in the literature [23–26]. A further miniaturization of these antennas has not been reported. Little has been presented in literature on the underlying procedure of impedance matching and miniaturization. In this section, we present an empirical procedure inferred from the design of inverse parabolic step antennas. The purpose of this procedure is to produce an initial geometry which is close to optimal to minimize numerical simulation complexity and time. We will then apply it to propose a new UWB antenna from the IPSS family to verify the application.

### 3.1. Useful Empirical Ratio and Values

#### *3.1.1. CPW Feed*

As a starting point, a square substrate is assumed (later detailed numerical analyses can result in a slightly off-square geometry). Refer to Fig. 1, if we define $w_a$ as the width of the antenna and $l_f$ as the length of the central feed of the CPW then we have found that an optimum impedance match occurs in the region of,

$$\frac{l_f}{w_a} \approx 0.35 \tag{3}$$

As $w_a = 30\,\text{mm}$ and 16 mm for the experimental models of the IPSS and Reflected IPSS antennas respectively, the values of $l_f$ for these designs according to the above equation should be 10.5 mm and 5.6 mm. As can be observed in Fig. 1, these values are in close agreement ($< 1\%$) to the actual values of 10.6 mm and 5.6 mm (resulting from detailed numerical optimization).

The empirical ratio given by the Equation (3) holds true for IPSS based antennas only. However, there is another family of CPW fed square shaped planar UWB antennas reported by Kim et al. [1, 27]

where a different ratio of $\frac{l_f}{w_a}$ has been used. Although not explicitly reported by the authors, for their proposed family of antennas a constant value of $\frac{l_f}{w_a} \approx 0.27$ has been used. Now recently, the authors of [28] have proposed another antenna from the same family as [1, 27] but using a different substrate. Quite interestingly, they have used nearly the same ratio of $\frac{l_f}{w_a} = 0.26$. This implies a generalization for the existence of a constant ratio of $\frac{l_f}{w_a}$ for a particular family of CPW fed UWB antennas. Due to the complex electromagnetic nature of the devices an analytic proof of this is not trivial.

The CPW center feed line to the side ground separation for IPSS and Reflected IPSS antennas have been kept at 0.33 and 0.39 mm. In later simulations we had found that increasing this distance to 0.59 mm maximum did cause an improvement in the VSWR performance of these antennas. Moreover, the separation of the main radiating element from the ground planes should be close to 0.4 mm. The width of the central feed should be kept in the range 3.6–3.8 mm. Following the central feed a small horizontal straight line, marked as n on Figs. 1(a) and (b), of length 0.6–0.9 mm should be used.

### *3.1.2. Inverse Parabolic Step Sequence*

Determining the IPSS is important not only for impedance matching but also for the overall length of the antenna. The empirical approach to selecting initial design of antenna is based on the study of the functions in Equations (1) and (2) and the straight lines which connect the start and end points of these curves.

The layout for the empirical approach to select the parabolic sequence is illustrated in Fig. 4 and Fig. 5. We start by considering the straight line $L_0$ connecting the start point of the first curve, i.e., $y_a$ to the end point of the last curves, i.e., $y_d$. According to the conventional equation of a straight line, $y(x) = mx + c$, the slope, $m_0$, of this line should lie in a specific range. This slope range is predicted from the trend present in the slopes of similar lines in the IPSS and Reflected IPSS antennas. For an antenna smaller than the reference geometry, $m_0$ should be $\geq 1$. Now consider the equation set (1) and (2). Here again, we get, by observing the trends in the slopes of the lines connecting start and end points of each curve in these two equations, the ranges for the slopes of similar lines in smaller antennas. For an antenna smaller than our reference antenna, i.e., the Reflected IPSS antenna these slope ranges in order should be: $m_a = 5.4 - 5.5$, $m_b = 0.2 - 0.3$, $m_c = 8 - 10$ and $m_d = 0.3 - 0.4$.

As can be observed that there are only two type of functions,

i.e., $y = x^2 + \alpha$ and $y = \tau\sqrt{x} + \theta$ alternating in both the equation sets (1) and (2). We can determine the length of the central feed from Equation (3) and by keeping its width in the prescribed range we can derive $P_0(x_0, y_0)$ the coordinates of the initial point of the first curve. These coordinates give us the value of $\alpha$ and $c$. Solving these equations will yield the coordinates of the end point of the first curve/start point of the second curve in the set. Moreover, the approximate formulation

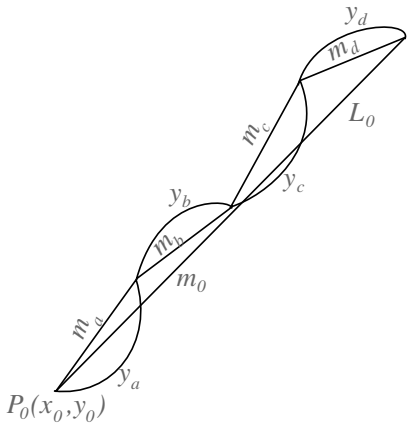


**Figure 4.** Empirical approach to calculating the Inverse Parabolic Step Sequence.

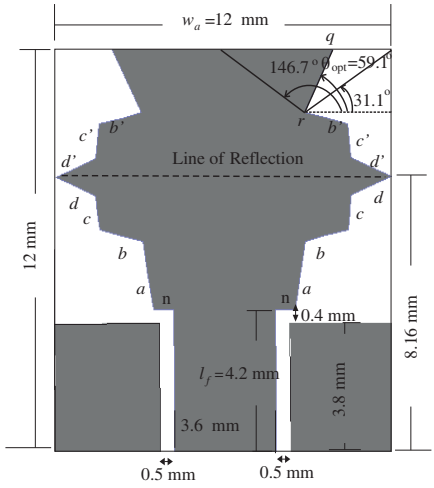


**Figure 5.** $\pi$-hat IPSS Antenna.

predicts the values of $\tau$ as $\geq 1$ for the second curve and $\geq 1.7$ for the fourth curve. Having known the start points and the equations of curves and straight lines connecting the ends, we can solve for the entire parabolic step sequence. We will then check whether the slope $m_0$ is $\geq 1$. As a variant, a partially reflected geometry is then chosen for the main radiating element as shown in Fig. 5. This is discussed in the following sub-section.

### 3.2. Further Miniaturized UWB Antenna: Application of the Empirical Design Rules

To show the utility of our proposed miniaturization empirical rules and formulation, we will propose an antenna smaller than our reference geometry of Fig. 1(b). Starting with an antenna size of 12 mm $\times$ 12 mm $\times$ 1.575 mm, we get from Equation (3) the length of central feed, $l_f = 4.2$ mm. Following the procedure in sub-section 3.1 we choose an initial value of the central feed width as 3.6 mm, ground to feed separation at 0.5 mm and distance of the radiating element from ground planes at 0.4 mm. From these, we get the ground planes width and the coordinates of the start point, $P_0(x_0, y_0)$ of the IPSS. From the empirical projection ranges we keep the values of line slopes as $m_a = 5.4$, $m_b = 0.26$, $m_c = 8.9$ and $m_d = 0.40$. We also select values of $\tau = 1$ for the second curve $y_b$ and $\tau = 1.8$ for the fourth curve $y_d$. The equation of the sequence becomes:

$$\begin{array}{ll} y_a(x) = x^2 - 2.05, & 2.5 \leq |x| \leq 2.872 \\ y_b(x) = \sqrt{x} + 4.505, & 2.872 \leq |x| \leq 4.388 \\ y_c(x) = x^2 - 12.656, & 4.388 \leq |x| \leq 4.501 \\ y_d(x) = 1.8\sqrt{x} + 3.878, & 4.501 \leq |x| \leq 5.912 \end{array} \quad (4)$$

The antenna is shown in Fig. 5. The sequence is marked as $a$-$d$ on the antenna. It can be observed that curves $b$, $c$ and $d$ are reflected in the line $y = 8.16$ to form curves $b'$-$d'$.

A final step is to complement the antenna geometry by optimizing the angle $\theta$ or the slope $\tan\theta$ of the line $\overline{rq}$ shown in Fig. 5. Considering line $\overline{rq}$, if point $r$ is fixed and $q$ is moved along the top edge of the substrate this varies the angle $\theta$. When $q$ is at the top right corner of the edge, the line $\overline{rq}$ (and its reflected image in the $y$-axis or the line $x = 0$) would form a pi/trapezium top section of antenna. At this point $\theta = 31.1°$. As $q$ moves from the top right corner to the mid-point of the top edge of the antenna, line $\overline{rq}$ (and its reflected image in $y$-axis) would form a pointed/triangular top section of the antenna. At this point $\theta = 146.7°$. An optimum angle $\theta_{opt} = 59.1°$ is achieved for best impedance match from the range 31.1°–146.7° as shown in Fig. 5.

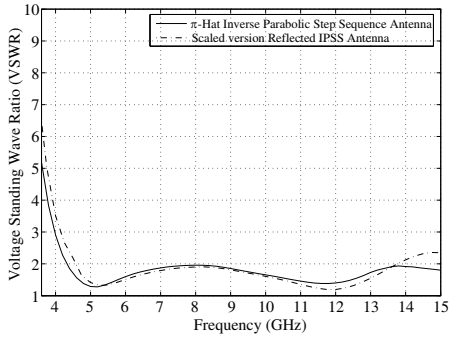


**Figure 6.** VSWR performance of $\pi$-hat IPSS Antenna.

From here we get the equation of the optimized straight line $\overline{rq}$ given as below:

$$y(x) = 1.67x + 5.319, \quad 2.872 < x < 4$$

The resulting section of the antenna forms a $\pi$-hat shape. The VSWR of the antenna is shown in Fig. 6. A VSWR $< 2$ over a frequency range of 4.2–15 GHz can be observed. If, instead of using this partially reflected geometry, we use purely reflected or scaled geometry as in case of Fig. 1(b), a 12.8% reduction in percentage bandwidth is observed as shown by Fig. 6.

## 4. AN ELECTRICAL MINIATURIZATION LIMIT

It can be calculated that the Reflected IPSS antenna is $0.16\lambda$ with reference to its lowest operating frequency of 3.0 GHz and has a percentage bandwidth of 127.3%. The $\pi$-hat antenna is $0.168\lambda$ (increase of 5%) and has a percentage bandwidth of 112.5%. As expected, we achieved miniaturization at the cost of percentage bandwidth [22] as lowest matched frequency has moved from 3.0 GHz to 4.2 GHz. As the dimensions of the Reflected IPSS antenna are 16 mm $\times$ 16 mm $\times$ 1.575 mm or its volume being 403.2 mm$^3$ and the dimensions of the $\pi$-hat antenna are 12 mm $\times$ 12 mm $\times$ 1.575 mm or its volume being 226.8 mm$^3$, it is a reduction in volume by an amount of 43.75%. However, a physical size reduction by an amount of 43.75% as compared to a loss in percentage bandwidth of 14.8% is a reasonable compromise. In another study to further establish the limit of electrical miniaturization for this family of antennas, an antenna size of 8 mm $\times$ 6 mm $\times$ 1.575 mm with same substrate was again simulated in HFSS. The lowest matched frequency in this case was found to be

6.0 GHz reinforcing the figure of $0.16\lambda$. This is indicative of a lower miniaturization limit of $0.16\lambda$ for IPSS based antennas.

## 5. CONCLUSION

In this paper we present an empirical approach to the miniaturization of IPSS based UWB antennas. The approach is derived from the study of the parabolic curves and the lines which subtend them. The empirical formulae derived for the IPSS class of antennas have been applied to produce a more compact form, termed as the $\pi$-hat IPSS antenna. In this paper we have also given a lower limit to the electrical size of the IPSS based antennas.

## REFERENCES

1. Kim, K.-H. and S.-O. Park, "Analysis of the small band- rejected antenna with the parasitic strip for UWB," *IEEE Transactions on Antennas and Propagation*, Vol. 54, No. 6, 1688–1692, Jun. 2006.
2. Balakrishnan, J., A. Batra, and A. Dabak, "A multi-band OFDM system for UWB communication," *2003 IEEE Conference on Ultra Wideband Systems and Technologies*, 354–358, Nov. 2003.
3. Batra, A., S. Lingam, and J. Balakrishnan, "Multi-band OFDM: a cognitive radio for UWB," *2006 IEEE International Symposium on Circuits and Systems, ISCAS, Proceedings*, 4, 2006.
4. Schantz, H., "UWB magnetic antennas," *IEEE Antennas and Propagation Society International Symposium*, Vol. 3, 604–607, Jun. 22–27, 2003.
5. Bahadori, K. and Y. Rahmat-Samii, "A miniaturized elliptic-card UWB antenna with wlan band rejection for wireless communications," *IEEE Transactions on Antennas and Propagation*, Vol. 55, No. 11, 3326–3332, Nov. 2007.
6. Mao, S.-G. and S.-L. Chen, "Frequency- and time-domain characterizations of ultrawideband tapered loop antennas," *IEEE Transactions on Antennas and Propagation*, Vol. 55, No. 12, 3698–3701, Dec. 2007.
7. Chen, D. and C.-H. Cheng, "A novel compact ultra-wideband (UWB) wide slot antenna with via holes," *Progress In Electromagnetics Research*, Vol. 94, 343–349, 2009.
8. Barbarino, S. and F. Consoli, "UWB circular slot antenna provided with an inverted-L notch filter for the 5 GHz WLAN band," *Progress In Electromagnetics Research*, Vol. 104, 1–3, 2010.

9. Marynowski, W. and J. Mazur, "Design of UWB coplanar antenna with reduced ground plane," *Journal of Electromagnetic Waves and Applications*, Vol. 23, No. 13, 1707–1713, 2009.
10. Kim, D.-O., N.-I. Jo, D.-M. Choi, and C.-Y. Kim, "Design of the ultra-wideband antenna with 5.2 GHz/5.8 GHz band rejection using rectangular split-ring resonators (SRRS) loading," *Journal of Electromagnetic Waves and Applications*, Vol. 23, No. 17–18, 2503–2512, 2009.
11. Ojaroudi, M., "Printed monopole antenna with a novel band-notched folded trapezoid for ultrawideband applications," *Journal of Electromagnetic Waves and Applications*, Vol. 23, No. 17–18, 2513–2522, 2009.
12. Zheng, Z.-A., Q.-X. Chu, and T.-G. Huang, "Compact ultra-wideband slot antenna with stepped slots," *Journal of Electromagnetic Waves and Applications*, Vol. 24, No. 8–9, 1069–1078, 2010.
13. Xiao, J. X. and M. F. Wang, "A novel UWB circinal slot antenna with band-stop characteristics," *Journal of Electromagnetic Waves and Applications*, Vol. 24, No. 8–9, 1125–1133, 2010.
14. Xia, Y.-Q., J. Luo, and D.-J. Luo, "Novel miniature printed monopole antenna with dual tunable band-notched characteristics for UWB applications," *Journal of Electromagnetic Waves and Applications*, Vol. 24, No. 13, 1783–1793, 2010.
15. Elsharkawy, Z. F., A. A. Sharshar, S. M. Elhalafawy, and S. M. Elaraby, "Ultra-wideband A-shaped printed antenna with parasitic elements," *Journal of Electromagnetic Waves and Applications*, Vol. 24, No. 14–15, 1909–1919, 2010.
16. Chu, Q.-X. and Y.-Y. Yang, "3.5/5.5 GHz dual band-notch ultra-wideband antenna," *Electronics Letters*, Vol. 44, No. 3, 172–174, Jan. 31, 2008.
17. Deng, C., Y. J. Xie, and P. Li, "CPW-fed planar printed monopole antenna with impedance bandwidth enhanced," *IEEE Antennas and Wireless Propagation Letters*, Vol. 8, 1394–1397, 2009.
18. Yin, K. and J. Xu, "Compact ultra-wideband antenna with dual bandstop characteristic," *Electronics Letters*, Vol. 44, No. 7, 453–454, Mar. 27, 2008.
19. Saleem, R. and A. Brown, "Inverse parabolic step sequence ultra wideband antenna," *Antennas Propagation Conference, 2009 LAPC Loughborough*, 773–775, Nov. 2009.
20. Saleem, R. and A. K. Brown, "Electrically small band-notch reflected inverse parabolic step sequence ultra wideband antenna,"

*2010 Proceedings of the Fourth European Conference on Antennas and Propagation (EuCAP)*, 1–3, Apr. 2010.

21. Kan, H., A. Abbosh, R. Waterhouse, and M. Bialkowski, "Compact broadband coplanar waveguide-fed curved quasi-yagi antenna," *Microwaves, Antennas Propagation, IET*, Vol. 1, No. 3, 572–574, Jun. 2007.
22. Mehdipour, A., A. Parsa, A.-R. Sebak, and C. Trueman, "Miniaturised coplanar waveguide-fed antenna and band-notched design for ultra-wideband applications," *Microwaves, Antennas Propagation, IET*, Vol. 3, No. 6, 974–986, Sep. 2009.
23. Yang. Y.-Y., Q.-X. Chu, and Z.-A. Zheng, "Time domain characteristics of band-notched ultrawideband antenna," *IEEE Transactions on Antennas and Propagation*, Vol. 57, No. 10, 3426–3430, Oct. 2009.
24. Pancera, E., D. Modotto, A. Locatelli, F. Pigozzo, and C. De Angelis, "Novel design of UWB antenna with band-notch capability," *2007 European Conference on Wireless Technologies*, 48–50, Oct. 2007.
25. Kim, Y. and D.-H. Kwon, "CPW-fed planar ultra wideband antenna having a frequency band notch function," *Electronics Letters*, vol. 40, No. 7, 403–405, Apr. 2004.
26. Lee, C.-M., T.-C. Yo, C.-H. Luo, W.-S. Chenh, C.-H. Tu, and Y.-Z. Juang, "Ultra-wideband printed disk monopole antenna with dual-band notched functions," *IEEE Annual Conference on Wireless and Microwave Technology, WAMICON'06*, 1–4, Dec. 2006.
27. Kim, K.-H., Y.-J. Cho, S.-H. Hwang, and S.-O. Park, "Band-notched UWB planar monopole antenna with two parasitic patches," *Electronics Letters*, Vol. 41, No. 14, 783–785, Jul. 2005.
28. Kim, D.-O. and C.-Y. Kim, "CPW-fed ultra-wideband antenna with triple-band notch function," *Electronics Letters*, Vol. 46, No. 18, 1246–1248, Sep. 2010.